كلية الهندسة

جامعة أسيوط

DESIGN AND ASSESSMENT OF A SPEED-BASED INTEGRATED ACTIVE VEHICLE CONTROLLER FOR LATERAL STABILITY

Mokhtar Al-Bukair, M-Emad S Soliman, S.M. Ahmed

Department of Mechanical Engineering, Assiut University, Egypt

ABSTRACT

An integrated active vehicle control system implementing fuzzy-logic control (FLC) is introduced. The system integrates three commercially- available active vehicle control systems, namely, Active Front Steering (AFS), Electronic Stability Control (ESC) and Torque Vectoring System (TVS) aiming at enhancing vehicle handling and cornering stability and rollover prevention. Two different vehicle models were constructed to simulate the dynamic behavior of the system with and without the proposed integration controller, namely, a 14-DOF vehicle dynamic model with nonlinear tire characteristics and a 2DOF bicycle reference model. Last model was utilized to generate controller's reference values of vehicle's yaw rate and body side slip angle at a given forward speed and driver's steering input. Simulation was carried out in the MATLAB/SIMULINK software environment. System effectiveness was investigated applying five different standard cornering test maneuvers at different vehicle forward speeds of 10, 20 and 30m/s. Simulated test maneuvers are: step, J-turn, single lane change (SLC), sine with dwell, (SWD) and fishhook. Results reveal that, for stability enhancement, AFS is most effective at low vehicle speeds with declining efficacy as speed goes up. Both ESC and TVS have been found to be equally effective at moderate to high speeds. However, due to the intrusive nature of ESC, TVS is considered to be the favored stability control mechanism. In conclusion, an integrated chassis control (ICC) strategy has been proposed that improves vehicle handling and cornering performance across the entire operating range of speed using

a forward-speed-based stability criterion to allocate stability control authority and ensure smooth transition of control between the three AFS, ESC, and TVS systems.

Keywords: Integrated Chassis Control (ICC), vehicle stability, Active Front Steering (AFS), Electronic Stability Control (ESC), Torque Vectoring System (TVS), Fuzzy Logic Control (FLC), MATLAB / SIMULINK, Cornering Test maneuvers.

1. Introduction

Vehicle stability enhancement has become crucial to every modern vehicle. A traditional road vehicle possesses three manual controls available for a human driver to control the dynamics of his vehicle. These are: throttle pedal control, brake pedal control and steering wheel control. The first two are primarily concerned with the longitudinal dynamics of the vehicle, while the third adjusts lateral movement (directional control). When the driving task is left solely to the driver, with no active intelligent assistance, vehicle performance is critically affected by the driver's psychology, response time and driving experience [1-4]. Under complex scenarios, such as driving at high speeds on slippery roads, in severe weather conditions, or handling sudden or difficult maneuvers; the risk of vehicle instability, leading to catastrophic accidents, increases. In such situations, dynamic auto-intervention or active control systems become extremely useful to avoid the potential for human error by avoiding and recovering from any unwanted disturbances in the path [1]. Active control systems are designed to help the driver by applying additional control actions or by modifying driver steer inputs. That is, in the entire vehicle system, the driver still functions as the primary controller and active control units are used as secondary or assistant units [5].

Nowadays, there is a large number of active dynamic controllers made available for vehicles to provide driver assistance and enhance passenger comfort, vehicle handling, stability and safety [6], [7]. In an active control, the control system replenishes driver action by sensing, complementing, and modifying it in a safe manner tending to handle the vehicle automatically. Vehicle active dynamic control systems are often categorized referring to the moving direction of the vehicle as: longitudinal, lateral, and vertical controls [1-3], [7]. Longitudinal control systems, such as ESC and TVS, automatically adjust braking and traction forces to improve vehicle performance and maintain vehicle stability. Examples of lateral control systems include AFS and Active Rear Steering (ARS). These systems come into effect in cornering situations to keep vehicle stability, correct under/over-steering and prevent roll-over. Active Suspension Systems (ASS) is the main and only vertical control system. An ASS is critical not only to passenger comfort, but also for vehicle stability and safety as it maintains tire-road contact and grip, without

which all other controls lose their functionality and become totally ineffective. However, ASS differs from other longitudinal and lateral active systems in that it solely handles the vertical dynamics automatically with no driver intervention.

Vehicle dynamic control systems are designed and made by different manufacturers and use different technologies and components to accomplish various control objectives and functionalities. When operated separately or individually, two major problems arise in such a parallel vehicle control architecture:

- The need for both software and hardware increase dramatically.
- Performance discrepancies arise between systems as vehicle dynamics in the three directions are coupled.

To dislodge these problems, an approach called "integrated vehicle dynamics control" was proposed in the 1990s that coordinates all chassis control systems and components to improve overall vehicle performance including safety, comfort and economy [1], [7]. At present, a large amount of research has focused at improving the vehicle's lateral dynamics. Most of these rely on regulating tire forces in both lateral and longitudinal directions, such as AFS, ESC and TVS. Many researchers have studied the integration of two systems [8-16], three systems [17-21], and four systems [1], [22-24]. Many control methods can be found in the literature, such as fuzzy logic control (FLC) [9], [10], [16-19], [21], sliding mode control (SMC) [11], [12], [17], [20], H∞ [1], [13], model predictive control (MPC) [14], [21], model-matching control (MMC)[8], nonsingular fast terminal sliding mode (NFTSM) [15], linear quadratic regulator (LQR) [22]. However, the subject of integrating control modules is still in the study phase and there are still parameters that need further studies.

The key contribution of this study is to enhance the stability of the vehicle by integrating three particular vehicle control systems: Active Front Steering (AFS), brake-based Electronic Stability Control (ESC) and driveline-based Torque Vectoring System (TVS). Five performance indicators; side slip angle, lateral acceleration, roll angle, yaw rate and dynamic load transfer ratio were used to evaluate vehicle stability. This paper is structured as follows: Section 1 is an introduction and a review of previous literature in the topic. Section 2 presents a detailed 14 DOF, passive vehicle dynamic model with a nonlinear tire model and a bicycle model, all developed in the MATLAB/Simulink environment. Section 3 introduces the proposed integrated FL control scheme. Sections 4 and 5 are devoted to the simulation results presentation and the final discussion and conclusion, respectively.

2. Vehicle System Models

In this paper, two different vehicle dynamic models were used: a main model and a reference model. The main model is a 14-DOF non-linear model used to precisely simulate vehicle's dynamic behavior. The reference model is a simplified, yet accurate, 2-DOF linear model used to calculate the desired responses to driver steering inputs [7].

2.1 Nonlinear vehicle model

In this model the sprung mass which comprises vehicle chassis, passengers and cargo, if any, is assumed to be perfectly rigid despite its large longitudinal and lateral dimensions. The model embodies five distinct rigid blocks; the vehicle body or sprung mass and four other identical unsprang masses representing wheel assemblies.
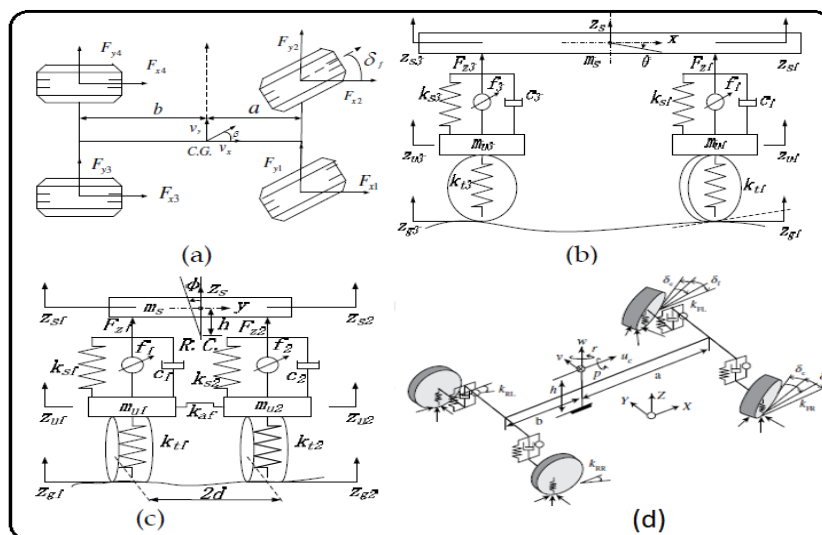

Fig. 1. Nonlinear vehicle dynamic mode

2.1.1. *Sprung mass dynamics*

The rigid sprung mass of the vehicle possesses a total of 6 DOF, three translational; Longitudinal, Lateral and Vertical and three rotational; Rolling, Pitching and Yawing. Its mathematical model may be written as:

➤ Longitudinal motion:

$$m(\ddot{x} - \dot{\psi}\dot{y} + \dot{\theta}\dot{z}) = (F_{xfl} + F_{xfr})\cos\delta - (F_{yfl} + F_{yfr})\sin\delta + (F_{xrl} + F_{xrr}) + m_s h_s \dot{\psi}\emptyset \quad (1)$$

➤ Lateral motion:

$$m(\ddot{y} + \dot{\psi}\dot{x} - \dot{\theta}\dot{z}) = (F_{xfl} + F_{xfr})\sin\delta + (F_{yfl} + F_{yfr})\cos\delta + (F_{yrl} + F_{yrr}) - m_s h_s \ddot{\emptyset} \quad (2)$$

➤ Vertical motion of sprung mass:

$$m_s(\ddot{z} - \dot{\theta}\dot{x} + \dot{\phi}\dot{}) = F_{szfl} + F_{szfr} + F_{szrl} + F_{szrr} - m_s g \tag{3}$$

> **Roll motion:**

$$I_{xx}\ddot{\phi} - I_{xz}(\ddot{\psi} + \dot{\phi}\dot{\theta}) + (I_{zz} - I_{yy})\dot{\theta}\dot{\psi}$$
$$= d(F_{szfl} - F_{szfr} + F_{szrl} - F_{szrr}) - m_s h_s a_y - m_s g\, h_s \sin\phi \tag{4}$$

> **Pitch motion:**

$$I_{yy}\ddot{\theta} + (I_{xx} - I_{zz})\dot{\phi}\dot{\psi} + I_{xz}(\ddot{\phi} - \ddot{\psi})$$
$$= -a(F_{szfl} + F_{szfr}) + b(F_{szrl} + F_{szrr}) - m_s h_s a_x \tag{5}$$

> **Yaw motion:**

$$I_{zz}\ddot{\psi} + (I_{yy} - I_{xx})\dot{\phi}\dot{\theta} + I_{xz}(\dot{\psi}\dot{\theta} - \ddot{\phi})$$
$$= a[(F_{xfl} + F_{xfr})\sin\delta + (F_{yfl} + F_{yfr})\cos\delta] - b(F_{yrl} + F_{yrr})$$
$$+ d[(F_{xfr} - F_{xfl})\cos\delta + F_{xrr} - F_{xrl}] \tag{6}$$

2.1.2. *Unsprung mass dynamics*

The presumed rigid masses of the wheel assemblies are attached to the vehicle body via the authentic suspension springs and dampers. Each wheel is assumed to have 2-DOF, one translational in the vertical displacement direction and another rotational in the wheel steering direction. All 4 wheels are assumed to be steerable. Equations of motion for unsprung masses can be derived as follows:

$$m_{ui}\ddot{z}_{ui} = F_{tzi} - F_{szi} \qquad where\ (i = fl, fr, rl\ and\ rr) \tag{7}$$

$$F_{tzi} = K_{ti}(z_{gij} - z_{uij}) + C_{ti}(\dot{z}_{gij} - \dot{z}_{uij}) \quad where\ (i = fl, fr, rl\ and\ rr) \tag{8}$$

$$F_{szfl} = K_{sfl}(z_{ufl} - z_{sfl}) + C_{Sfl}(\dot{z}_{ufl} - \dot{z}_{sfl}) + \frac{K_{af}}{2d}\left[\phi - \frac{z_{ufl} - z_{ufr}}{2d}\right] + F_{fl} \tag{9}$$

$$F_{szfr} = K_{sfr}(z_{ufr} - z_{sfr}) + C_{Sfr}(\dot{z}_{ufr} - \dot{z}_{sfr}) - \frac{K_{af}}{2d}\left[\phi - \frac{z_{ufl} - z_{ufr}}{2d}\right] + F_{fr} \tag{10}$$

$$F_{szrl} = K_{srl}(z_{url} - z_{srl}) + C_{Srl}(\dot{z}_{url} - \dot{z}_{srl}) + \frac{K_{ar}}{2d}\left[\phi - \frac{z_{url} - z_{urr}}{2d}\right] + F_{rl} \tag{11}$$

$$F_{szrr} = K_{srr}(z_{urr} - z_{srr}) + C_{Srr}(\dot{z}_{urr} - \dot{z}_{srr}) - \frac{K_{ar}}{2d}\left[\phi - \frac{z_{url} - z_{urr}}{2d}\right] + F_{rr} \tag{12}$$

$$z_{sfl,r} = z_s - a\sin\theta \pm d\sin\phi \tag{13}$$

$$z_{srl,r} = z_s + b\sin\theta \pm d\sin\phi \tag{14}$$

$$z_{srr} = z_s + b\sin\theta - d\sin\phi \tag{15}$$

2.2.   Classical bicycle model

In general, the accuracy of a model is closely related to its complexity. However, due to the computational burden, it is often desired to use a simplified model, especially for active control. For this reason, further assumptions are introduced to reduce model complexity while maintaining the precision related to the control objectives. The resulting model is a 2-DOF model called a bicycle model. The bicycle vehicle model (also called single-track model) is a simplified planar model (in the x-y plane) describing the chassis' lateral and yaw dynamics of a dual-axle, single- rigid- body ground vehicle. The model represents a four-wheeled vehicle, with left and right wheels lumped into a single front and a single rear wheel. This model precisely encompasses many characteristics that are essential to the dynamics of the vehicle under many different conditions providing an effective mathematical framework to analyze the basic aspects of handling and stabilization of the vehicle. Essentially, it proved to be a valuable tool for designing effective vehicle chassis control systems [2], [25].
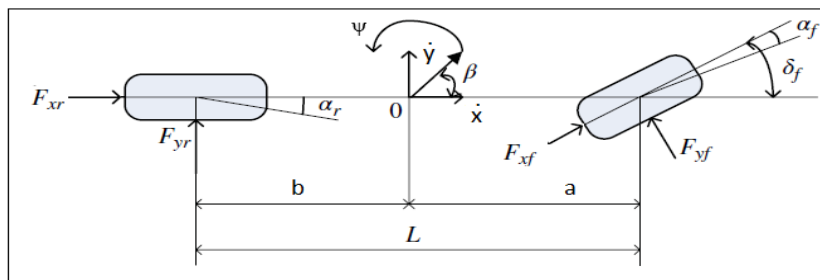

Fig. 2. 2DOF Bicycle (or Single-Track) Vehicle Model

Mathematical Formulation of the bicycle model is as follows:

$$\dot{X} = AX + BU$$
$$Y = CX + DU \tag{16}$$

Where X, U and Y are the system state, input, and output vectors respectively

$$X = \begin{bmatrix} \beta \\ \dot{\psi} \end{bmatrix} \qquad , \quad U = [\delta] \qquad , \quad Y = \begin{bmatrix} \beta \\ \dot{\psi} \end{bmatrix} \tag{17}$$

and A, B, C and D are the system, input, output and feed-forward matrices respectively:

$$A = \begin{bmatrix} A_{11} & A_{12} \\ A_{21} & A_{22} \end{bmatrix} = \begin{bmatrix} -2\left(\dfrac{C_{\alpha f} + C_{\alpha r}}{m\dot{x}}\right) & -2\left(\dfrac{C_{\alpha f}\,a - C_{\alpha r}\,b}{m\dot{x}^2}\right) - 1 \\ -2\left(\dfrac{C_{\alpha f}\,a - C_{\alpha r}\,b}{I_z}\right) & -2\left(\dfrac{C_{\alpha f}\,a^2 + C_{\alpha r}\,b^2}{I_z\dot{x}}\right) \end{bmatrix} \,,$$

$$B = \begin{bmatrix} B_1 \\ B_2 \end{bmatrix} = \begin{bmatrix} 2\left(\dfrac{C_{\alpha f}}{m\,\dot{x}}\right) \\ 2\left(\dfrac{C_{\alpha f}\,a}{I_z}\right) \end{bmatrix} \quad , C = \begin{bmatrix} 1 & 0 \\ 0 & 1 \end{bmatrix} \quad , \; D = [0] \tag{18}$$

Model inputs are vehicle speed and steering wheel angle. Model outputs are the desired lateral stability criteria: yaw rate, sideslip angle, lateral acceleration, etc. In steady state, the desired values of the vehicle sideslip angle and yaw rate, are expressed as follows [7], [15], [24], [26]

- Desired sideslip angle

$$\beta_{des} = \frac{b - \dfrac{a\,m\dot{x}^2}{2C_{\alpha r}(a + b)}}{a + b + \dot{x}^2\,k_{us}} \times \delta_d \tag{19}$$

- Desired yaw rate

$$\dot{\psi}_{des} = \frac{\dot{x}}{a + b + \dot{x}^2\,k_{us}} \times \delta_d \tag{20}$$

where k_{us} is the understeer coefficient and is defined as

$$k_{us} = m\left(\frac{b\,C_{\alpha r} - a\,C_{\alpha f}}{2(a + b)C_{\alpha f}C_{\alpha r}}\right) \tag{21}$$

To limit lateral forces resulting from large lateral accelerations, the upper limits of the yaw rate and side slip angle are suggested as [15], [24], [26], [27S]:

$$\dot{\psi}_{uber\;bound} = 0.85\frac{\mu g}{\dot{x}} \tag{22}$$

$$\beta_{upper\;bound} = \tan^{-1}(0.02\,\mu g) \tag{23}$$

The 2-DOF linear vehicle model actually reflects the relationship between the yaw rate and steering angle, therefore it is used as a reference model [18].

2.3. Tire model

This paper uses the empirical model of the magic formula of tire proposed by Pacejka, using the formulae of trigonometric functions combined with real tire data. Tire parameters are given in Table (1).

$$F_{x0i} = D_x \sin\{C_x \tan^{-1}[B_x x - E_x(B_x x - \tan^{-1} B_x x)]\} + S_{vx} \tag{24}$$

$$x = \lambda + S_{hx} \tag{25}$$

$$F_{y0i} = D_y \sin\{C_y \tan^{-1}[B_y x - E_y(B_y x - \tan^{-1} B_y x)]\} + S_{vy} \tag{26}$$

$$x = \alpha + S_{hy} \tag{27}$$

$\lambda \equiv$ is a tire slip ratio;
$\alpha \equiv$ tire sideslip angle
$D =$ the crest factor,
$B =$ the curve origin slope,
$E =$ the curve form factor,
$C =$ the shape characteristic factor,
S_h, $S_v =$ are the Horizontal and Vertical drifts respectively [2], [24], [27].

$$\lambda = \frac{R_w \omega_{wi} - V_{wxi}}{\max(R_w \omega_{wi}, V_{wxi})} \tag{28}$$

The speed of each vehicle wheel in the rolling direction of the wheel is given by [28S], [29S]:

$$V_{wx_f} = (\dot{x} \pm d\dot{\psi}) \cos \delta_f + (\dot{y} + a\dot{\psi}) \sin \delta_f \tag{29}$$

$$V_{wx_r} = \dot{x} \pm d\dot{\psi} \tag{30}$$

$$\alpha_f = \delta_f - \tan^{-1}\left(\frac{\dot{y} + a\dot{\psi}}{\dot{x} \pm d\dot{\psi}}\right) \tag{31}$$

$$\alpha_r = -\tan^{-1}\left(\frac{\dot{y} - b\dot{\psi}}{\dot{x} \pm d\dot{\psi}}\right) \tag{32}$$

$$F_{nzfl} = \frac{b}{2(a+b)} mg - \frac{h_{cg}}{2(a+b)} ma_x - \frac{bh_{cg}}{2(a+b)d} ma_y + \frac{h_{cg}^2}{2(a+b)gd} ma_x a_y \tag{33}$$

$$F_{nzfr} = \frac{b}{2(a+b)} mg - \frac{h_{cg}}{2(a+b)} ma_x + \frac{bh_{cg}}{2(a+b)d} ma_y - \frac{h_{cg}^2}{2(a+b)gd} ma_x a_y \tag{34}$$

$$F_{nzrl} = \frac{a}{2(a+b)} mg + \frac{h_{cg}}{2(a+b)} ma_x - \frac{ah_{cg}}{2(a+b)d} ma_y - \frac{h_{cg}^2}{2(a+b)gd} ma_x a_y \tag{35}$$

1080

Mokhtar Al-Bukair et al., Design and Assessment of a Speed-Based Integrated Active Vehicle ….

$$F_{nzrr} = \frac{a}{2(a+b)}mg + \frac{h_{cg}}{2(a+b)}ma_x + \frac{ah_{cg}}{2(a+b)d}ma_y + \frac{h_{cg}^2}{2(a+b)gd}ma_xa_y \qquad (36)$$

$$I_w\dot{\omega}_{wi} = -F_{xwi}R_w + T_i , \qquad (i = fl, fr, rl, rr) \qquad (37)$$

$$T_i = T_{di} - T_{bi} , \qquad (38)$$

Table 1. Nonlinear Tire Parameters [30]

Parameter	symbol	(tracking) Value	(braking) Value
Longitudinal stiffness coefficient	B_x	$22 + \dfrac{F_z - 1940}{645}$	$22 + \dfrac{F_z - 1940}{430}$
Longitudinal shape factor	C_x	$1.35 + \dfrac{F_z - 1940}{16125}$	
Longitudinal crest factor	D_x	$2000 + \dfrac{F_z - 1940}{0.956}$	$1750 + \dfrac{F_z - 1940}{0.956}$
Longitudinal curvature coefficient	E_x	-3.6	0.1
Lateral stiffness coefficient	B_y	$2.2 + \dfrac{5200 - F_z}{4000}$	
Lateral shape factor	C_y	$1.26 + \dfrac{5200 - F_z}{32750}$	
Lateral crest factor	D_y	$-0.0003F_z^2 + 1.8096F_z - 22.73$	
Lateral curvature coefficient	E_y	-1.6	

3.Proposed Integrated Control Model

A coordinating control system, which integrates three fuzzy logic controllers namely, AFS control, TVS control and ESC control to enhance vehicle cornering stability is presented. In the integrated controller, shown in Fig(3), the AFS fuzzy logic controller calculates δc based on δd and e(ψ˙), ESC fuzzy logic controller calculates MESC based on e(ψ˙) and e(β), finally, TVS fuzzy logic controller calculates MTVS based on e(ψ˙) and e(β) .

- sideslip angle error:

$$e(β)=β\_des-β\_act \qquad (39)$$

- yaw rate error:

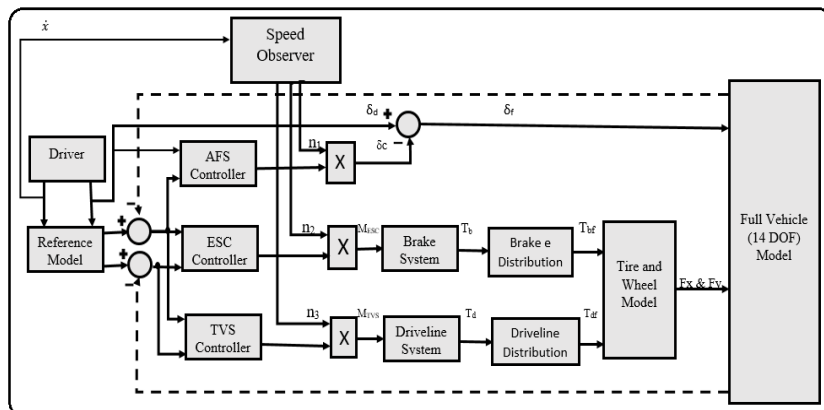$$e(ψ˙)=ψ˙\_des-ψ˙\_act \qquad (40)$$

Fig. 3. Schematic Diagram of the Proposed Integrated Controller.

Membership functions of the three active fuzzy logic controllers are given in Figs. 4 and 5. Fuzzy rules are given in Table 2. The Mamdani Fuzzy Inference Scheme (FIS) is used by the fuzzy controller and is defined by the following rules:

IF e(β) is A and e ($\dot{\psi}$) is B THEN (δc) is C $\qquad$ (for AFS controller)
IF e(β) is A and e ($\dot{\psi}$) is B THEN MTVS is C $\qquad$ (for TVS controller)
IF e(β) is A and e ($\dot{\psi}$) is B THEN MESC is C $\qquad$ (for ESC controller)
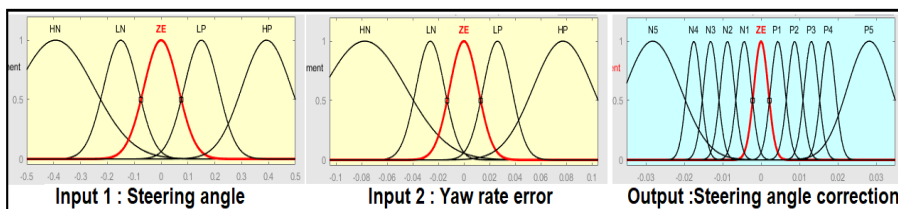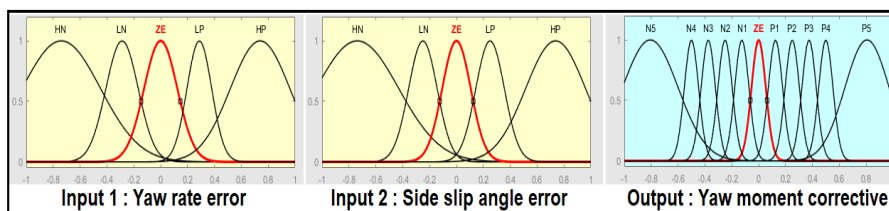

Fig. 4. Membership functions of the AFS controller

Fig. 5. Membership functions of the ESC and TVS controllers

3.1. TVS drive torque estimation unit sub model

This unit estimates the driving torque going to the front wheels based on the sign of the yaw-moment MTVS control signal.

$$T_{df} = \frac{MF*M_{TVS}*R_W}{(d \, \cos\delta_f - a\sin\delta_f)} \tag{41}$$

$$MF = \frac{F_{nzfl}+F_{nzfr}}{F_{nzfl}+F_{nzfr}+F_{nzrl}+F_{nzrr}} \tag{42}$$

Table 2. Fuzzy rule for the AFS, TVS and ESC controllers

1. Steering angle correction (δ_c), 2. Yaw moment corrective of TVS(M_{TVS}) 3. Yaw moment corrective of ESC(M_{ESC})		Yaw rate error ($e_{\dot\psi}$)				
		HN	**LN**	**ZE**	**LP**	**HP**
Sideslip angle error (e_β) or Steering angle (δ_d)	HP	N1	N1	ZE	P1	P1
	LP	N2	N2	ZE	P2	P2
	ZE	N3	N3	ZE	P3	P3
	LN	N4	N4	ZE	P4	P4
	HN	N5	N5	ZE	P5	P5

3.2. TVS drive torque allocation unit sub model

This unit decides which of the front wheels should receive driving torque, so that the wheels do not receive conflicting signals that could lead to vehicle instability. Allocation control base is given in Table 3.

Table 3. TVS allocation control base of driving torque to individual wheels

Yaw rate error $e_{\dot\psi} = \dot\psi_{des} - \dot\psi_{act}$	Apply driving torque to
$< 0 e_{\dot\psi}$	Front left wheel (FLW)
$> 0 e_{\dot\psi}$	Front right wheel (FRW)
$= 0 e_{\dot\psi}$	Neither (HOLD)

3.3. ESC brake torque estimation unit sub model

This unit estimates the braking torque directed to the front wheels based on the M_{ESC} yaw-control signal.

$$T_{bf} = \frac{MF*M_{ESC}*R_W}{(d \, \cos\delta_f - a\sin\delta_f)} \tag{43}$$

3.4. ESC brake torque allocation unit sub model

This unit specifies which particular front wheel must receive braking torque, so that the wheels do not receive mixed signals that could cause the vehicle to become unstable. Allocation control base is given in Table 4.

Table 4. ESC allocation control base of braking torque to individual wheels

Yaw rate error $= \dot{\psi}_{des}\text{-}\dot{\psi}_{act} e_{\dot{\psi}}$	Wheel steering angle δ_f	Status description	Apply braking to
$< 0 e_{\dot{\psi}}$	$\delta_f > 0$	Over steering	FRW
	$\delta_f < 0$	Under steering	FLW
$> 0 e_{\dot{\psi}}$	$\delta_f > 0$	Under steering	FLW
	$\delta_f < 0$	Over steering	FRW
$= 0 e_{\dot{\psi}}$	For all δ_f	Neutral steering	HOLD

3.5. Forward speed observer unit

Since both AFS, TVS and ESC are able to control the five performance indicators (side slip angle, lateral acceleration, roll angle, yaw ratio and dynamic load transmission ratio) and improve the vehicle's lateral stability to a certain extent. The operating regions of these systems must first be indicated (working range). Operating range limits can be determined using various vehicle dynamic parameters, such as side slip angle, lateral acceleration (abbreviated as "latac"), yaw angle, vehicle speeds and rates, etc. Published research on this topic reveals that AFS is effective in improving stability at low vehicle forward speeds (less than 10 m/s). Its efficacy declines afterwards. Both ESC and TVS are reported to be effective in vehicle stabilization at medium (between 10 and 30 m/s) and high (above 30 m/s) vehicle speeds. However, the intrusive nature of ESC advances TVS as the preferred mechanism for controlling stability. The input to this integration control module is the vehicle's forward speed and the outputs are n_1, n_2, n_3 ($n_1 + n_2 + n_3 = 1$).

3.6. Stability performance indicators

Five performance indicators were used to verify the vehicle's stability. The closer the values of these indicators to zero, the greater the stability of the vehicle. These indicators are:

- *Side slip angle* which is the angle between the direction the wheel is pointing and the direction it is going, that can be expressed by the equation below:

$$\beta = \tan^{-1}\frac{\dot{y}}{\dot{x}} \tag{44}$$

- *Lateral acceleration* functions normally to the vehicle's direction of motion. For example, when going around a bend it can be perceived as a centrifugal force to the outside of the bend.
- *Roll angle* is the vehicle's angle of rotation about its longitudinal axis. Rolling is mainly due to steering inputs and unequal roadway inputs between right and left wheels. The load is moved from the inner wheels to the outer wheels during rolling motion [24].

- *Yaw rate* of a vehicle is the angular speed of rotation about the vertical axis, or rate of change of the heading angle when the vehicle is horizontal.
- *Dynamic load transfer ratio LTR_d* is used to recognize a vehicle's rollover, it is given by the following equation [17], [19]:

$$LTR_d = \frac{F_{zfl} + F_{zfr} - F_{zrl} - F_{zrr}}{F_{zfl} + F_{zfr} + F_{zrl} + F_{zrr}} \qquad (45)$$

The LTR_d value must be between -1 and +1. Otherwise, the vehicle's right or left wheels have lost contact or are about to lose contact with ground and are at risk of rolling over [19], [27].

4. Results and Discussion

Simulation results are presented for five different cornering maneuvers, namely, step, J turn, single lane change, sine with dwell, and fishhook at three vehicles forward speeds of 10, 20 and 30 m/s. Nominal road friction coefficient is selected to be μ = 0.85, a value generally considered representative of dry paving [24]. Dynamic response to these maneuvers at the vehicle speeds is simulated and compared for 5 different arrangements, namely, the passive (uncontrolled vehicle), the individual AFS, ESC or TVS controlled vehicle, and finally the integrated control. Comparison is based on five performance indicators of stability, namely, side slip angle, lateral acceleration, roll angle, yaw rate, and dynamic load transfer ratio. Results show that AFS is effective at the speeds of 10 and 20 m/s while its effectiveness drops considerably at 30 m/s failing to prevent vehicle rollover. As for ESC and TVS, they show to be ineffective at the low speed of 10 m/s, especially in the side slip angle. Integrated control, on the other hand proved its effectiveness at all three speeds. Simulation results are presented in figures 6 through 25 below.

4.1. Step maneuver

For the step maneuver simulation, a step steering input (steering hand wheel angle) of 60 degrees (Fig. 6) has been applied at different vehicle forward speeds. Based on 5 performance indicators, results show that the efficacy of each independent controller varies widely at different vehicle speeds while the proposed integrated control (ICC) manages to improve and stabilize performance at all investigated input speeds. At a vehicle forward speed of 10 m/s (Fig. 7), both ESC and TVS show significant improvements in all performance indicators except one indicator, namely, the side slip angle. At this speed both AFS and ICC equally introduced improvements to all performance indicators. At 20 m/s (Fig. 8) the performance indicators are greatly improved with ICC, followed by AFS, then ESC and TVS come in third place with almost the same effect. At 30 m/s (Fig. 9), ESC and TVS are

superior but with sensible performance oscillation, followed by ICC which clearly introduces a more stable performance. However, due to tire force saturation, AFS has a very limited performance influence that approaches the passive system.
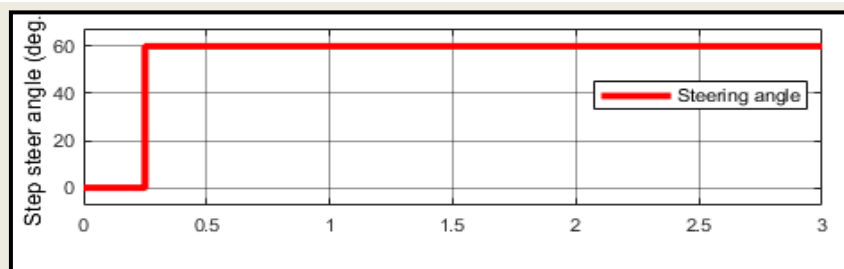
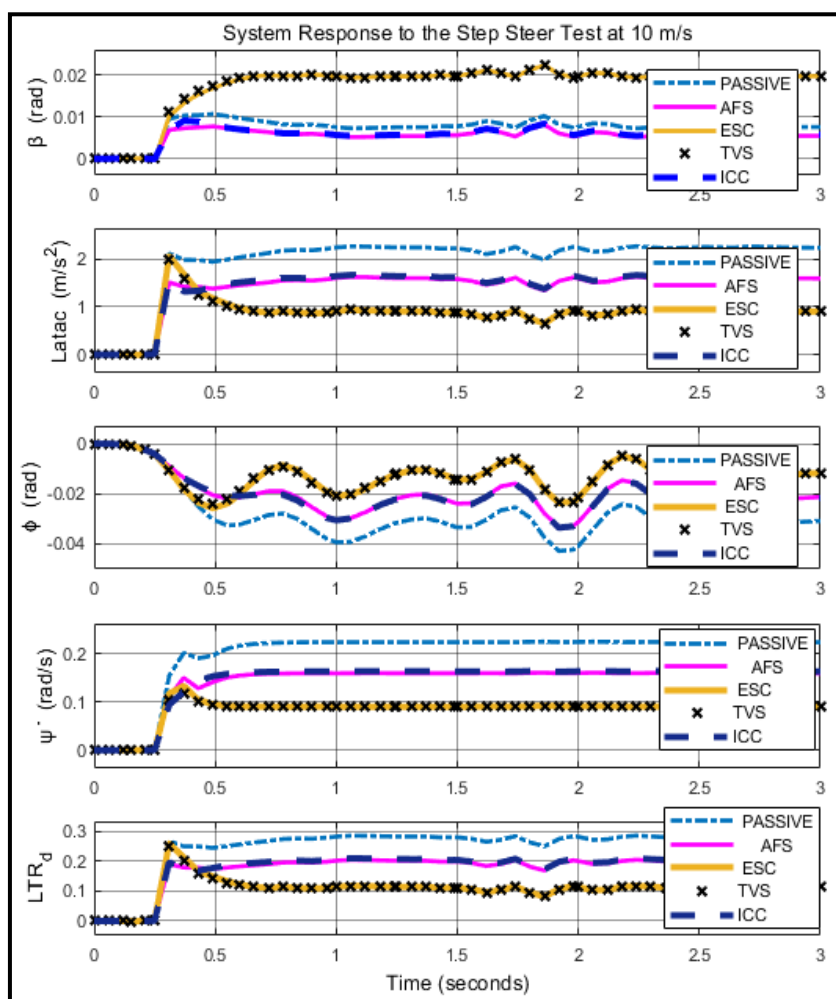

Fig. 6. Step steer maneuver
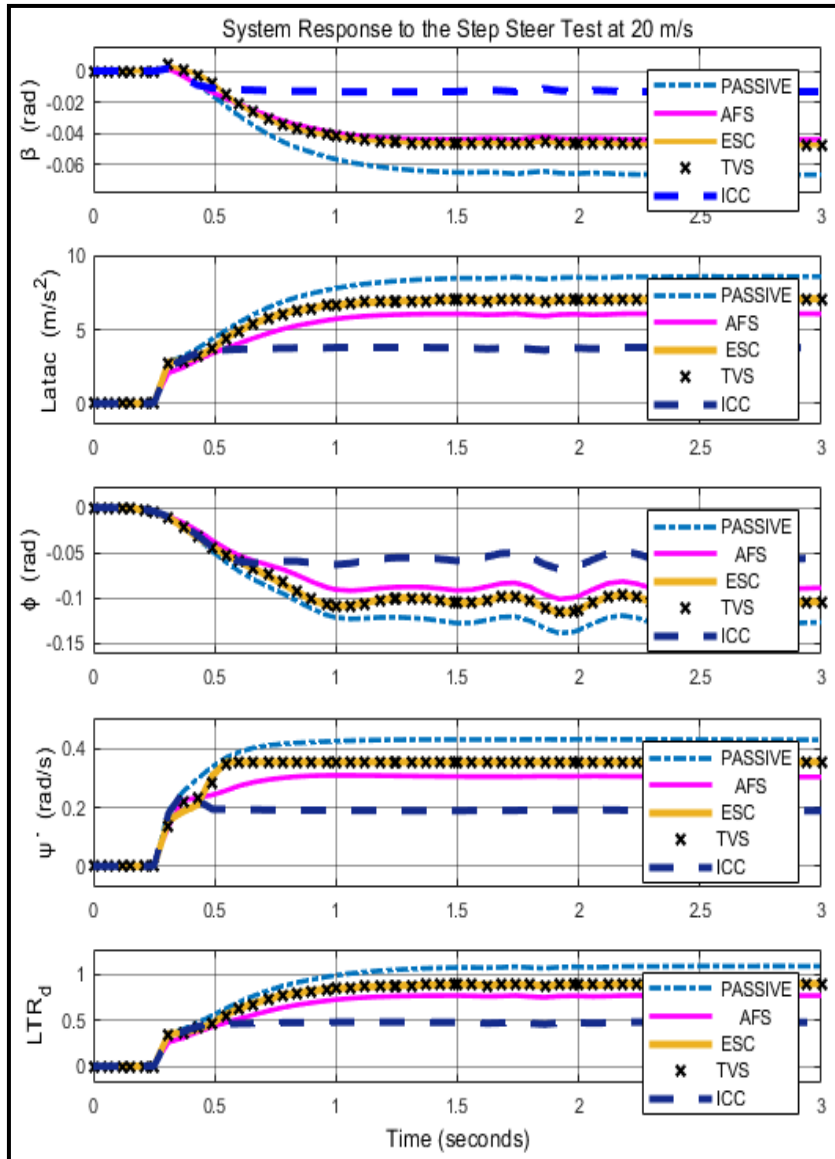

Fig. 7. System Response to the Step Steer Test at 10 m/s
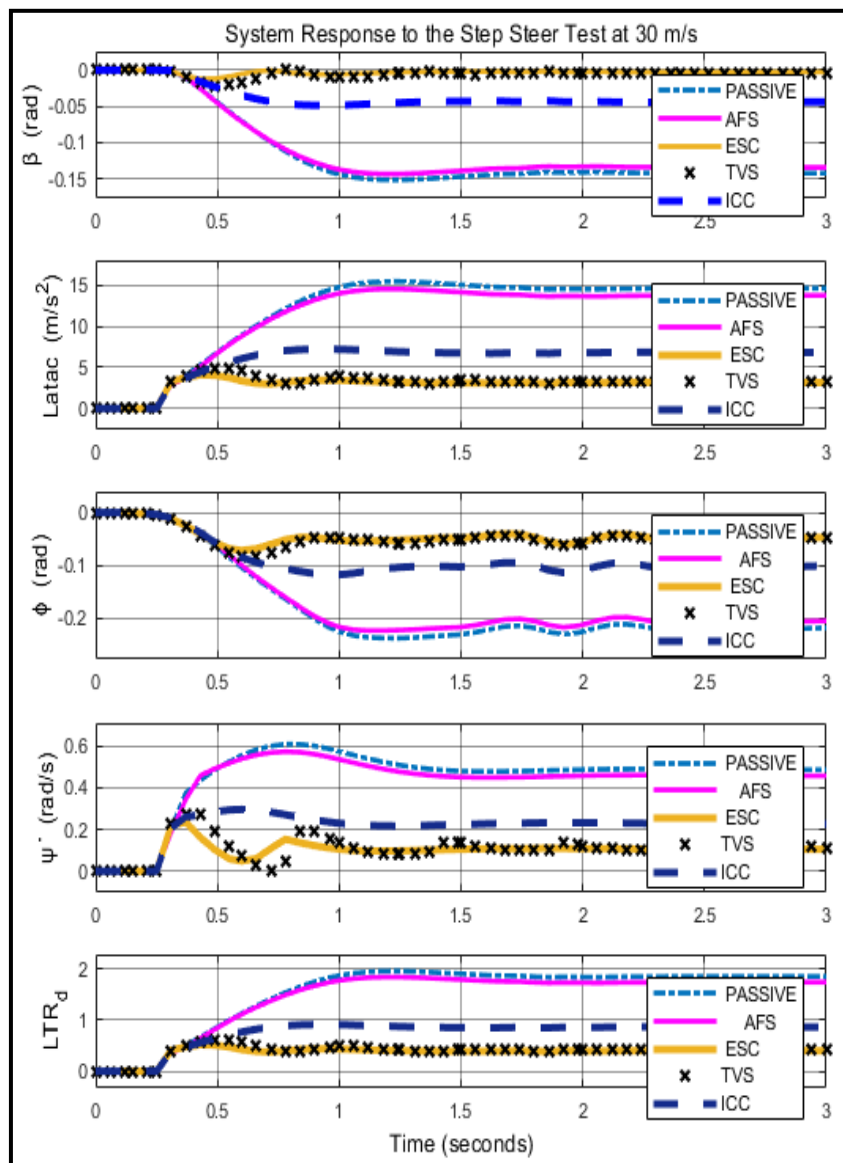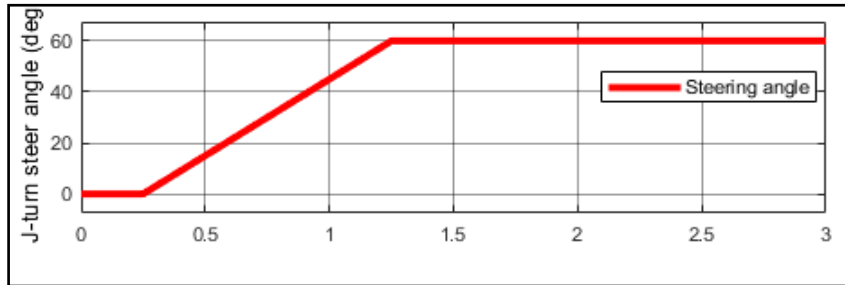
Fig. 8 System Response to the Step Steer Test at 20m/s.

Fig. 9. System Response to the Step Steer Test at 30 m/s

4.2. J-turn maneuver

The vehicle's response to J-turn maneuver (Fig. 10) with a maximum hand wheel angle of 60 degrees is shown in Figures 11 to 13. At 10 m/s, (Fig. 11), both ICC and AFS provide improvements in all performance indicators while he ESC and TVS have no influence on the side slip angle performance indicator. At 20 m/s, (Fig. 12), the ICC excels in improving all performance indicators, followed by AFS, ESC, and finally TVS. At 30 m/s, (Fig. 13), best improvement come with ESC and TVS, followed directly by the ICC. AFS

approaches the passive system and fails to prevent the vehicle from rolling over.
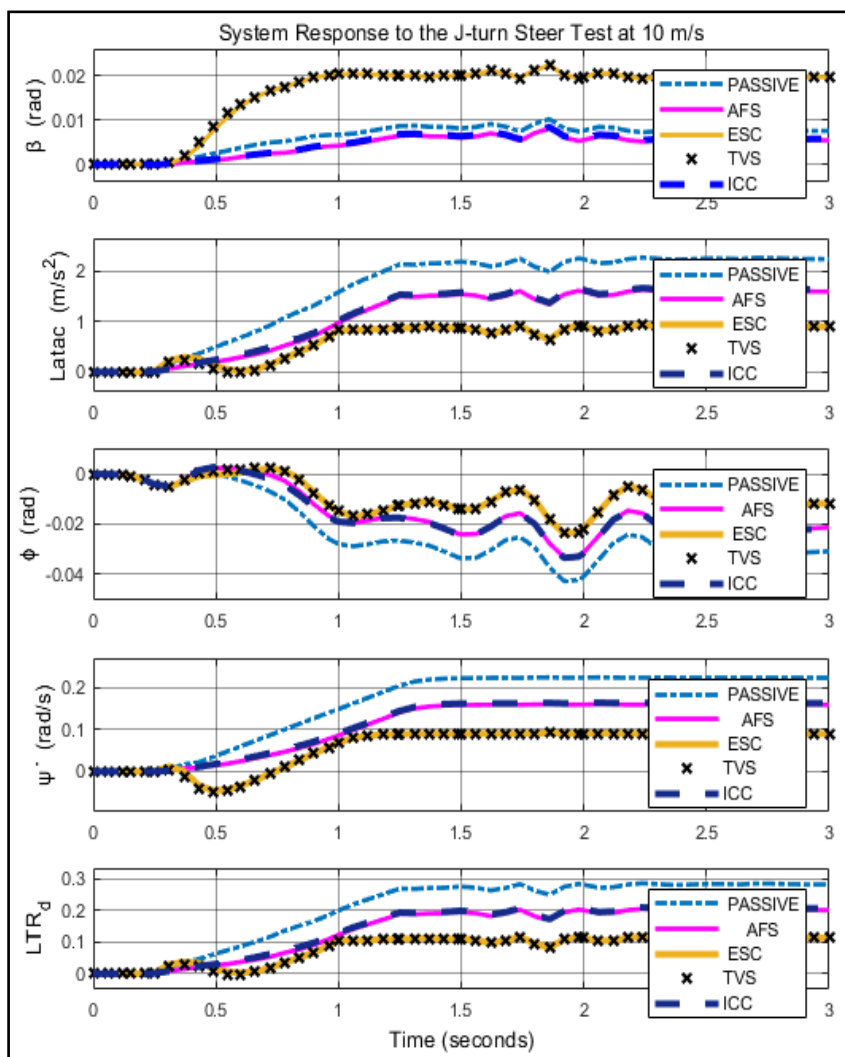

Fig. 10. J-turn steer maneuver

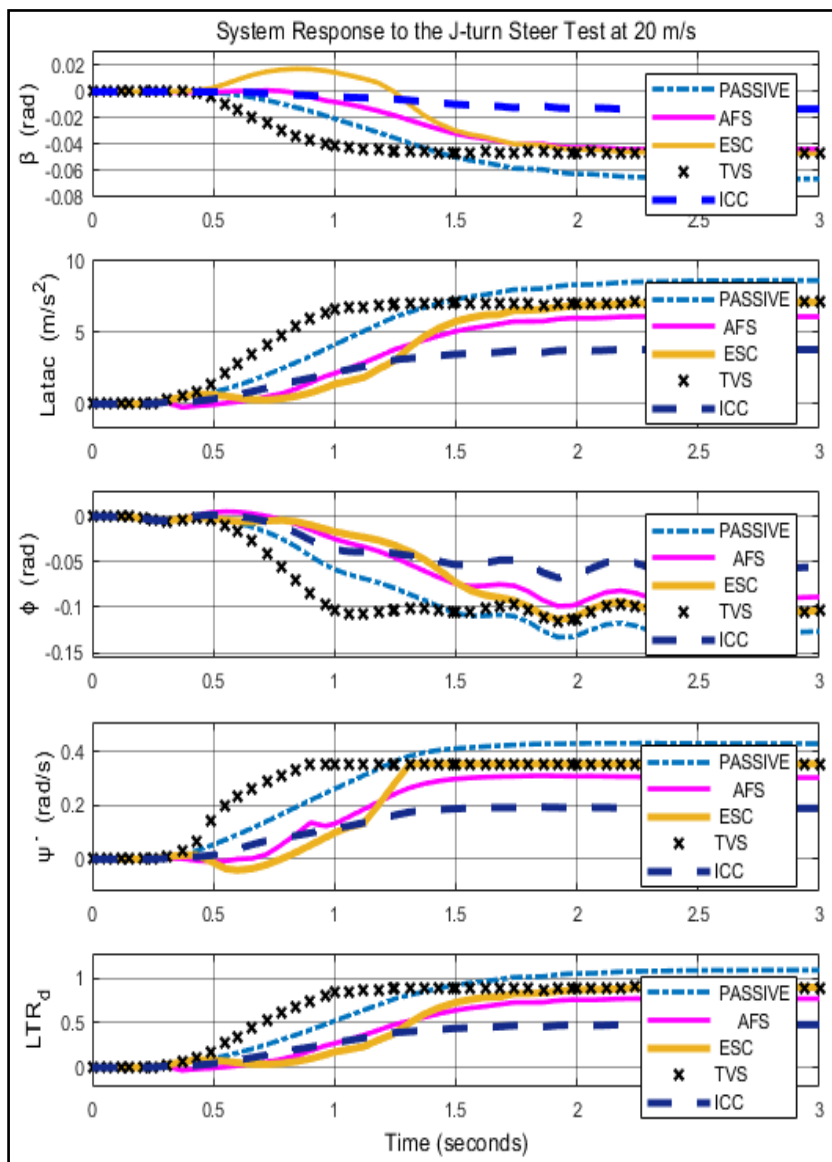Fig. 11. System Response to the J- turn steer test at 10 m/s.

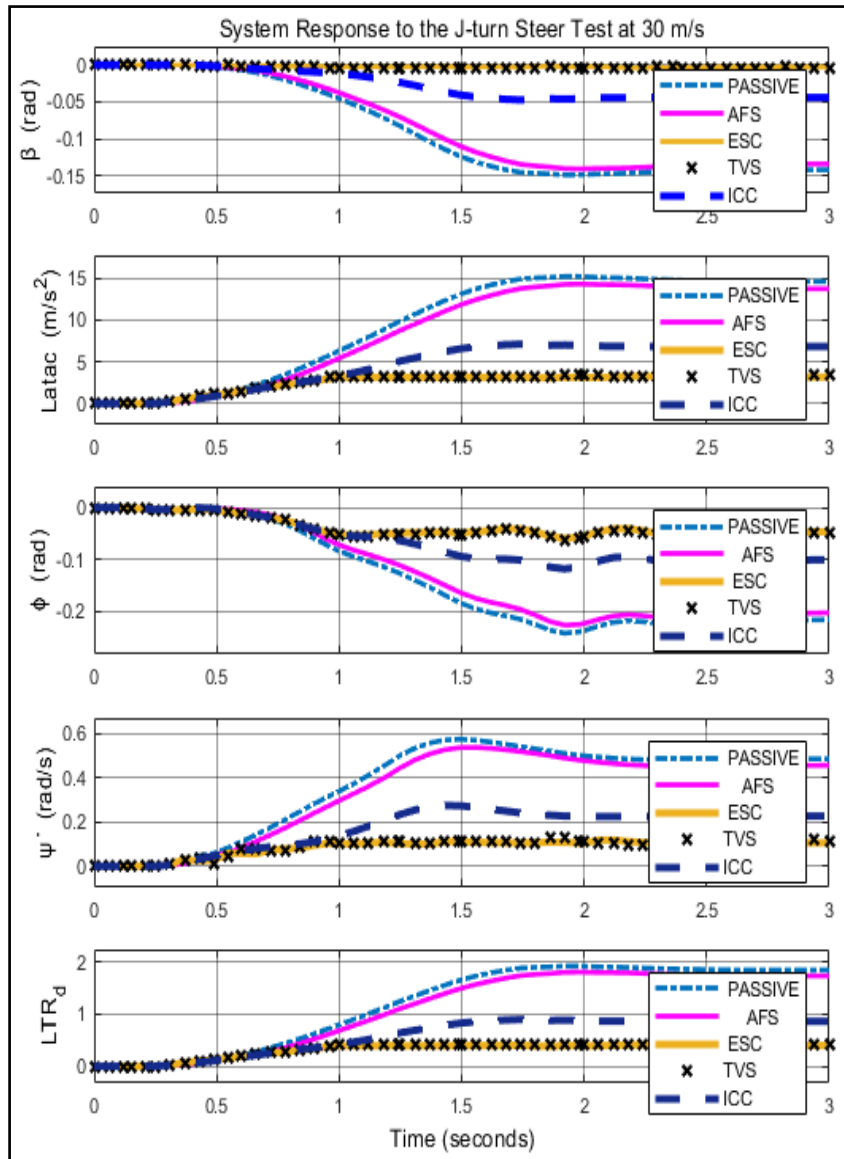Fig. 12. System Response to the J- turn steer test at 20 m/s.

Fig. 13. System Response to the J- turn steer test at 30 m/s.

4.3.   SLC maneuver

The vehicle's response to SLC maneuver (Fig. 14) with a maximum hand wheel angle of 40° is shown in Figures 15 to 17. At a speed of 10 m/s, (Fig. 15), good improvement is obtained with both ICC and AFS. ESC fails in the side slip angle performance indicator while TVS performs poorly. At 20 m/s, (Fig. 16), the ICC excels in improving the side slip angle and is more streamlined than other systems. At 30 m/s, (Fig. 17), ICC, ESC, and TVS perform identically

and show great improvement. As usual, AFS shows little improvement at higher speeds due to the saturation of tire forces.
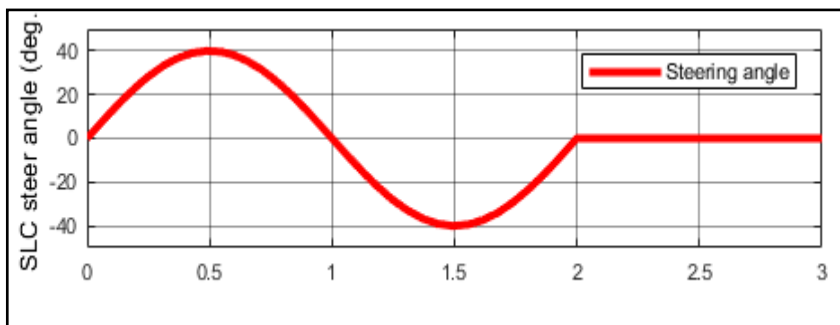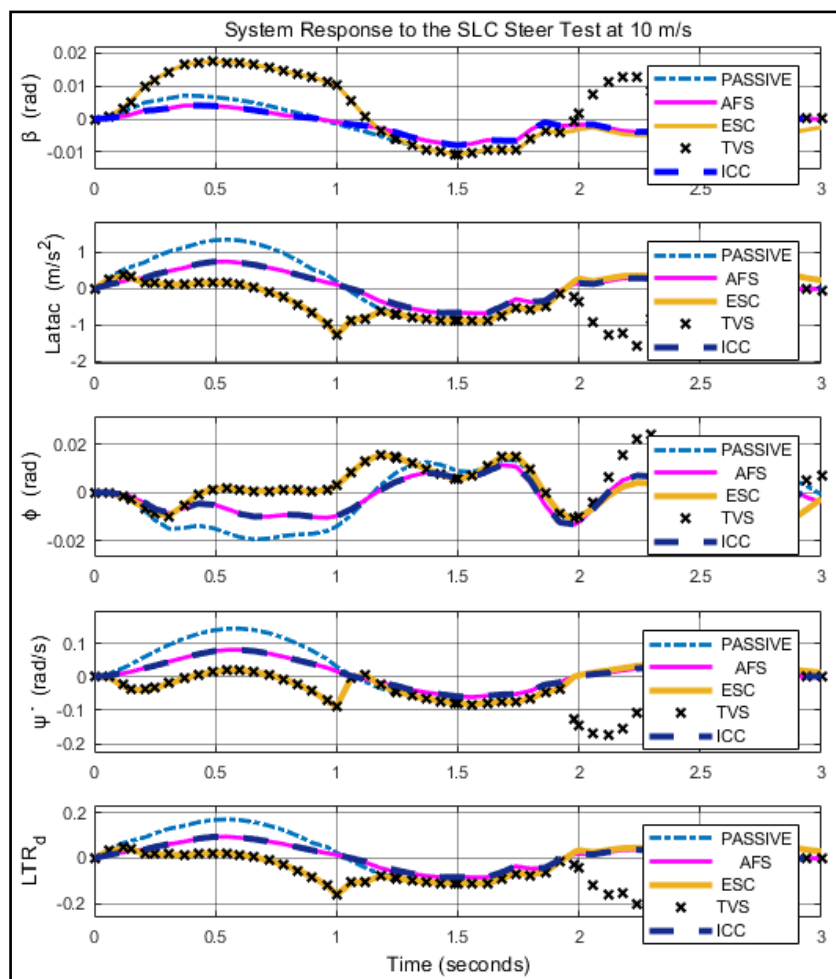

Fig. 14. SLC steer maneuver

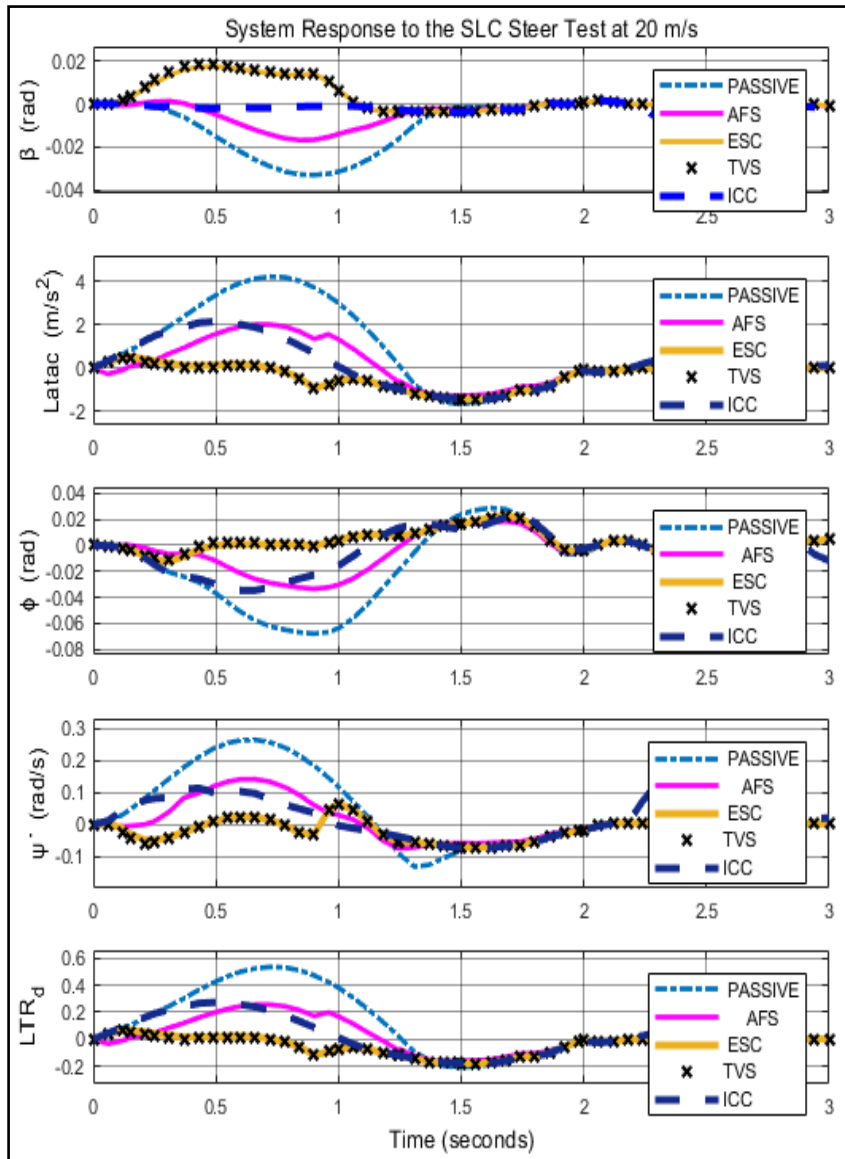Fig. 15. System Response to the SLC steer test at 10 m/s
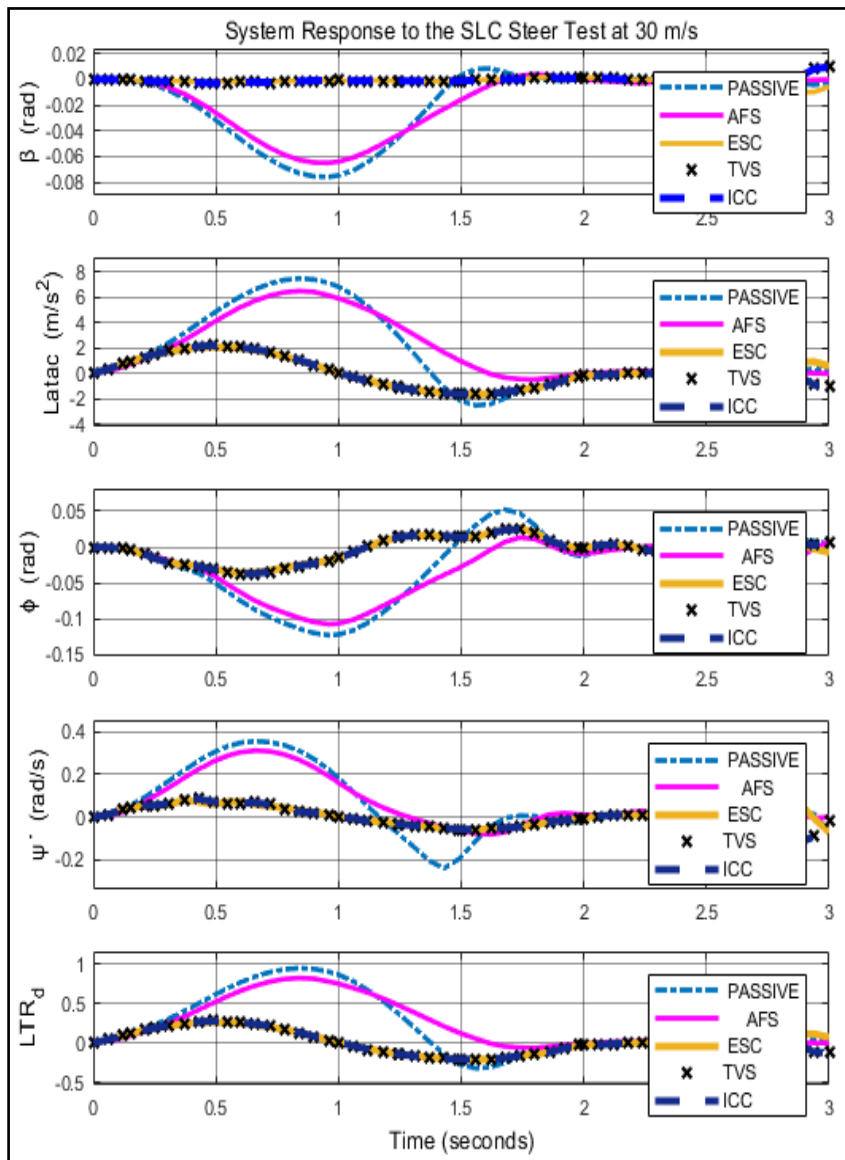
Fig. 16. System Response to the SLC steer test at 20 m/s

Fig. 17. System Response to the SLC steer test at 30 m/s

4.4. SWD maneuver

The vehicle's response to SWD maneuver (Fig. 18) with a maximum hand wheel angle of 80° is shown in Figures 19 to 21. At 10 m/s, (Fig.19), AFS and ICC improve performance equally, while ESC fails to improve side slip angle performance, and TVS performance is clearly poor. At 20 m/s, (Fig. 20), the ICC improves the performance especially in improving the lateral slip angle performance index and then the rest of the systems come out almost equally in the performance improvement. At 30 m/s, (Fig. 21), ICC, ESC and TVS show

significant improvement, while AFS shows a slight improvement at high speeds due to the saturation of tire forces.
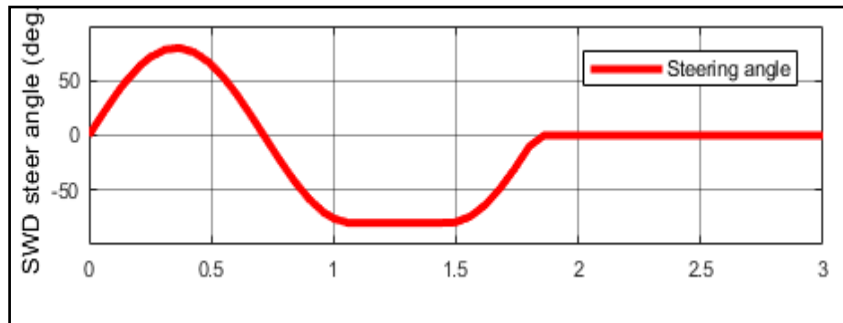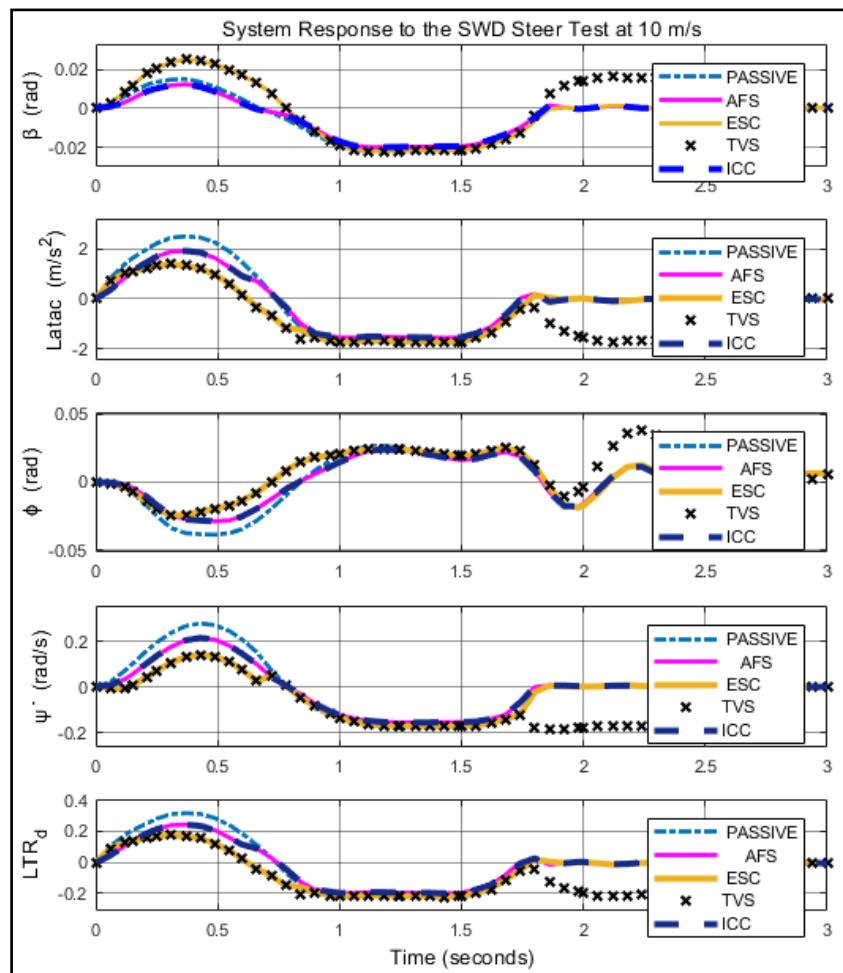

Fig. 18. SWD steer maneuver

Fig. 19. System Response to the SWD steer test at 10 m/s.
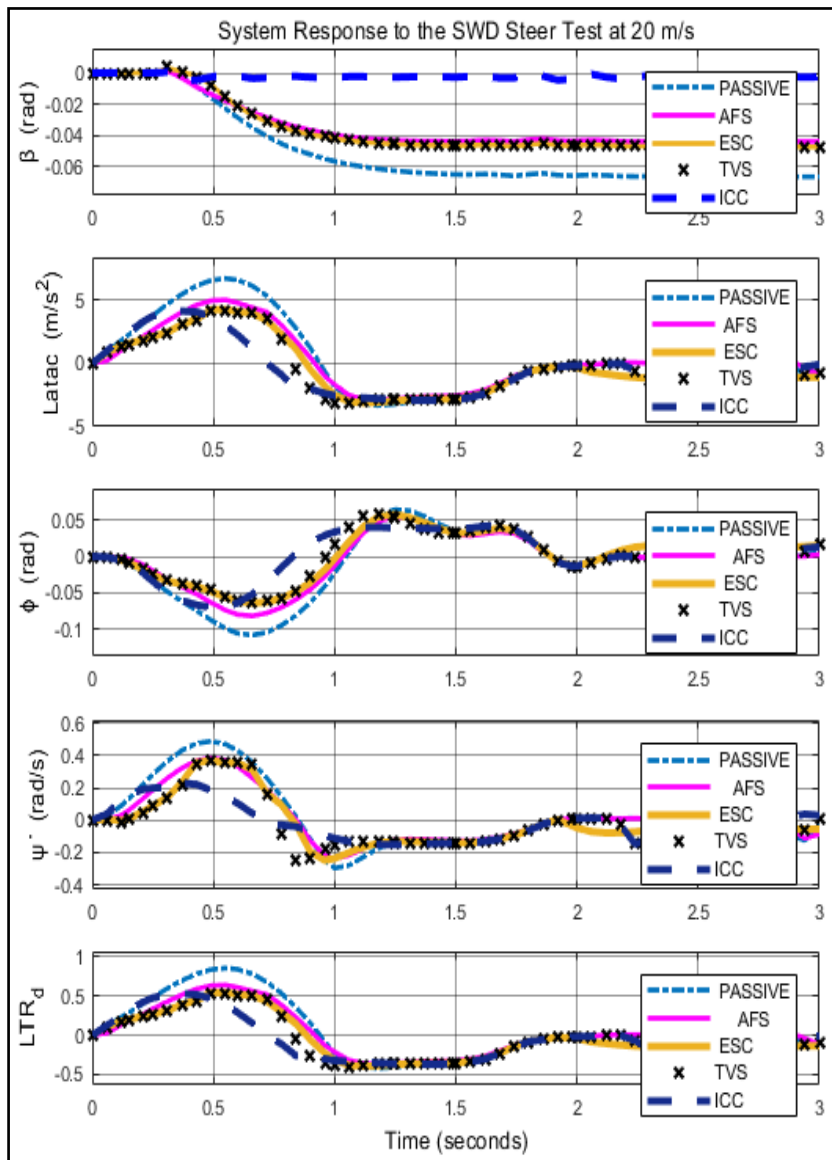
Fig. 20. System Response to the SWD steer test at 20 m/s.
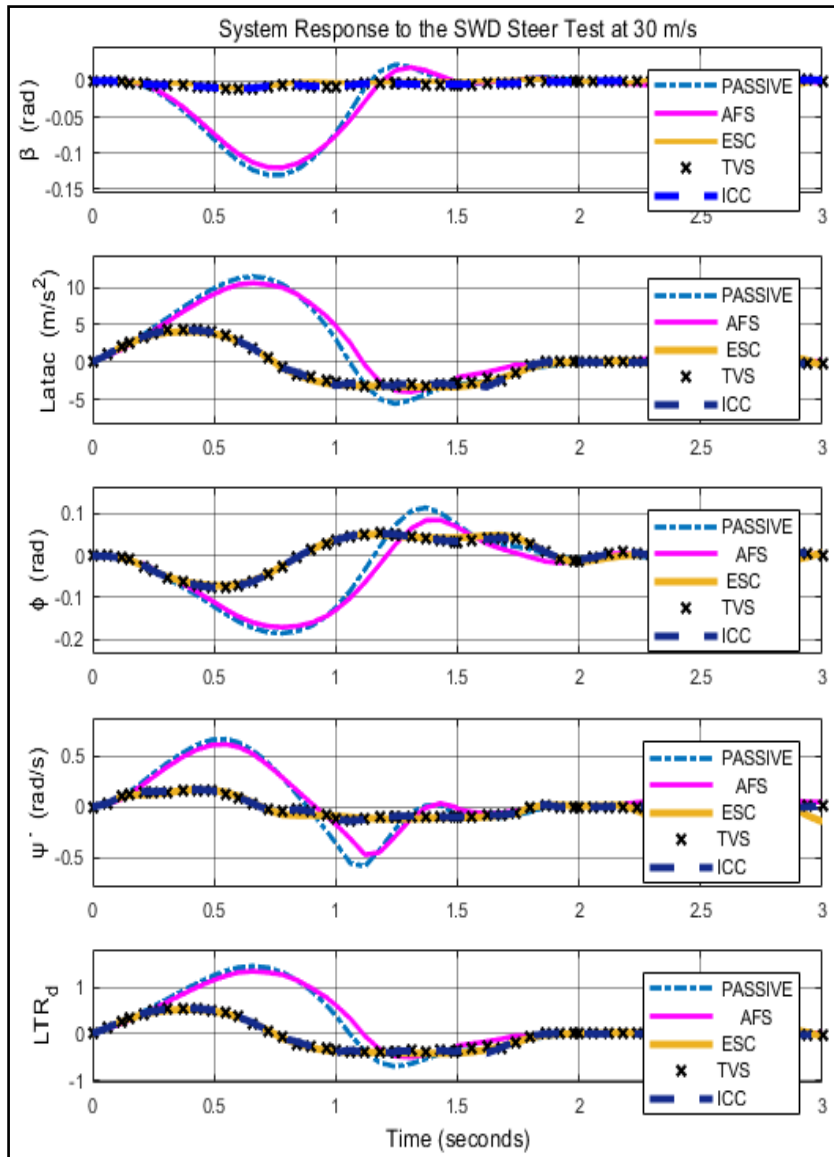
Fig. 21. System Response to the SWD steer test at 30 m/s.

4.5.   Fish hook maneuver

The vehicle's response to the fishhook maneuver (Fig. 22) with a maximum hand wheel angle of 60° is shown in Figures 23 to 25. At 10 m/s, (Fig. 23), there is an improvement for both ICC and AFS. However, ESC and TVS both fail the lateral slip angle performance index. At 20 m/s, (Fig. 24), ICC significantly performs in front of all other systems with AFS surpassing ESC and TVS in improving the performance indicators of side slip angle and yaw rate moment. However, TVS is found superior in improving the rest of

indicators. At 30 m/s, (Fig.25), ICC, ESC and TVS are identical in showing significant improvement. As usual, AFS shows little improvement and fails to prevent rollover.
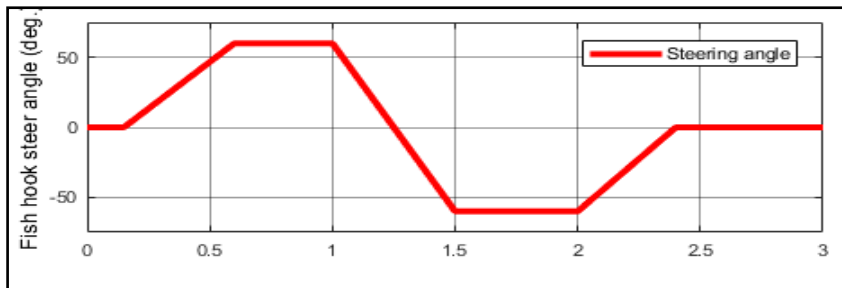
Fig. 22. Fish hook steer maneuver
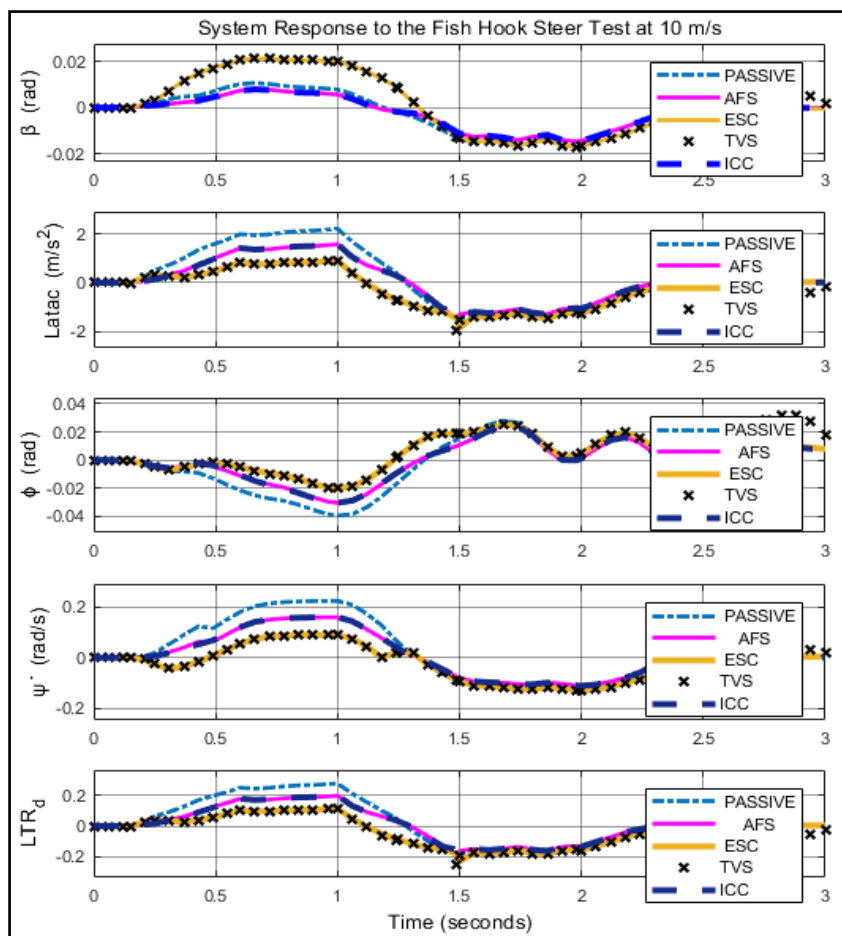
Fig. 23. System Response to the Fish hook steer test at 10 m/s.
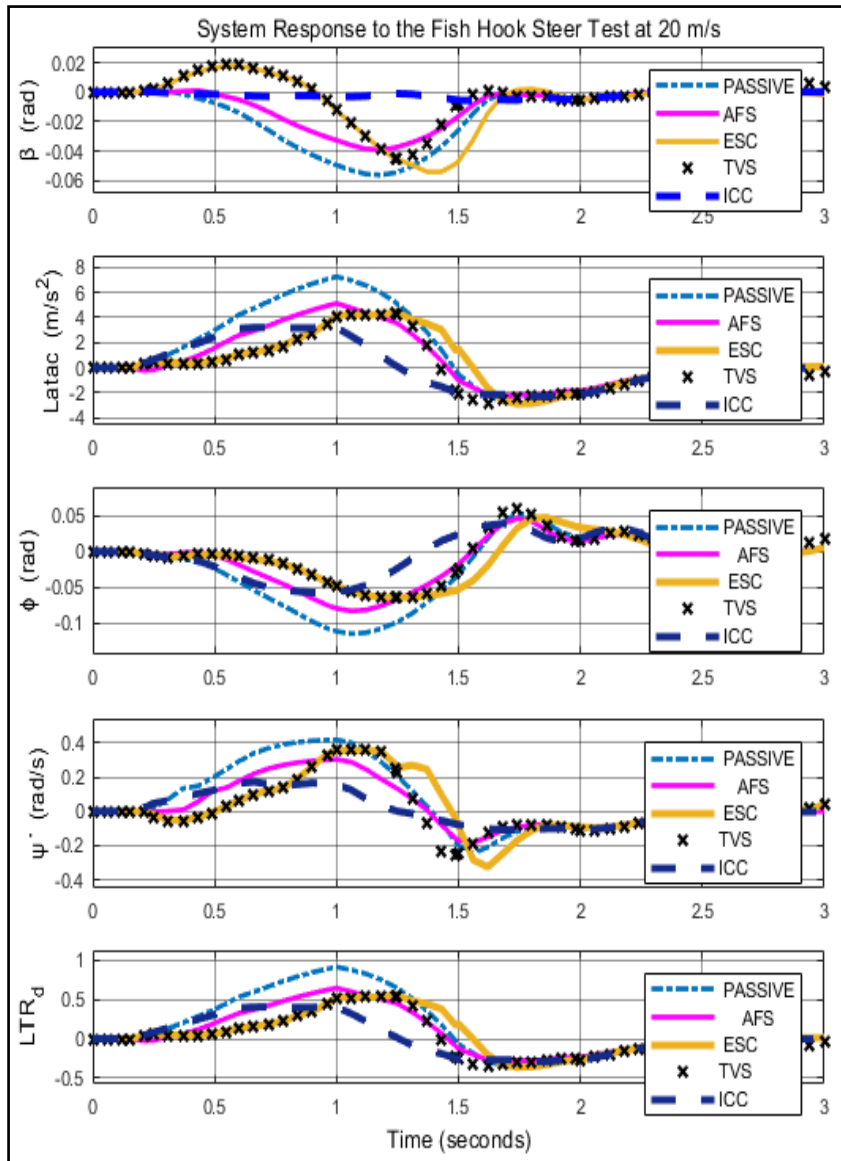
Fig. 24. System Response to the Fish hook steer test at 20 m/s.
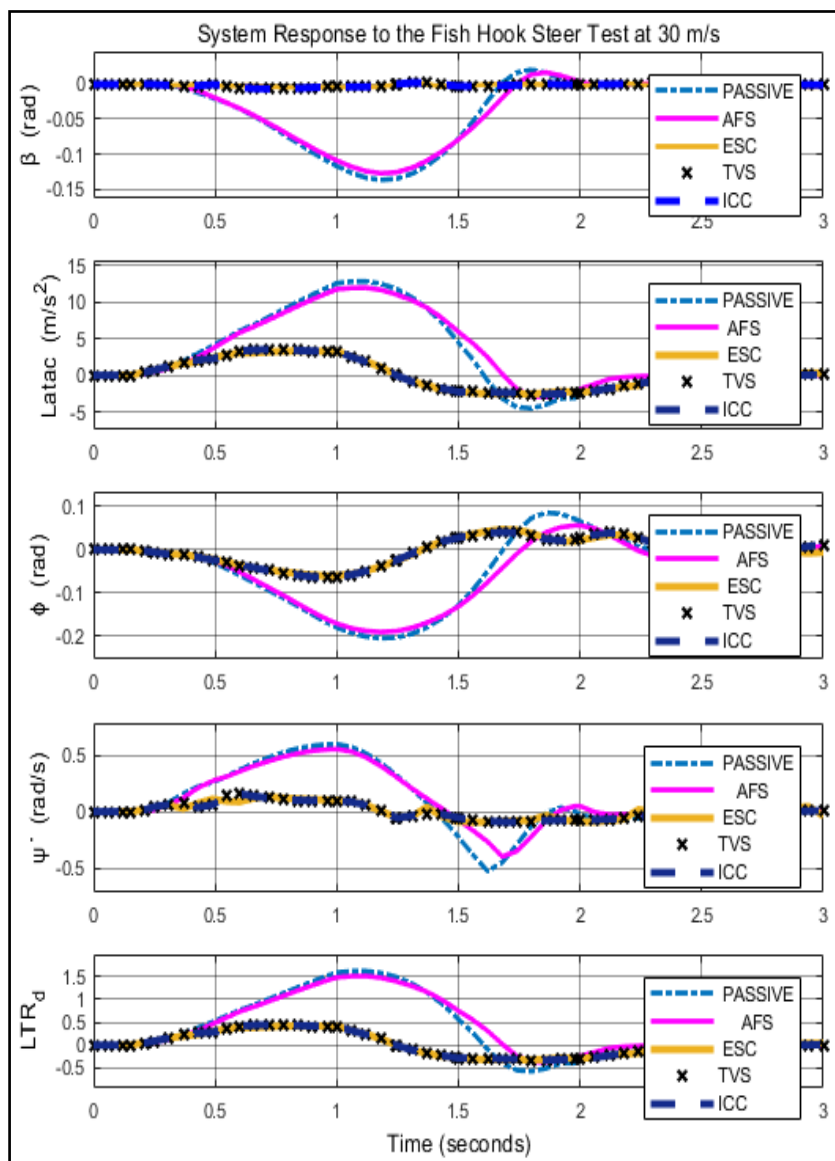
Fig. 25. System Response to the Fishhook steer test at 30 m/s.

6. Conclusions

The paper proposed an integrated control system that integrates AFS, ESC, and TVS to improve vehicle handling, stability and prevent rollover. The proposed control system generates corrective steering angle, braking torque and driveline torque. The performance of the proposed system was evaluated by numerical simulation of the vehicle model using MATLAB / Simulink. The control unit appears to be an effective means of controlling vehicle handling

and stability. FLC strategies have been used to control the three systems due to their effectiveness in controlling nonlinear systems. The simulation results show that the AFS is more effective in low forward speed, while the ESC and TVS is effective in all values of medium and high forward speed, and the vehicle with the proposed integrated control system has smaller side slip angle, yaw rate, roll angle, lateral acceleration and dynamic load transfer ratio than a passive control vehicle for step, J turn, single lane change, sine with dwell and fishhook steer inputs with three different vehicle speeds.

Appendix A. Parameters of system model

No.	Model parameters	symbol	value
	Dimensions (m)		
1.	Distance from vehicle CG to front axle	A	0.968
2.	Distance from vehicle CG to rear axle	B	1.392
3.	Half of the wheel track	D	0.64
4.	Distance between front and rear axles	L	2.36
5.	Dynamic wheel radius	R_w	0.280
6.	Vehicle focused mass to roll or pitch axle	h_s	0.505
7.	Vehicle centroid to ground height	h_{cg}	0.707
	Masses (kg)		
8.	Total vehicle mass	M	1030
9.	Vehicle sprung mass	m_s	810
10.	Vehicle un-sprung mass at front left/ front right corners	m_{us_fl}/m_{us_fr}	26.5
11.	Vehicle un-sprung mass at rear left/ rear right corners	m_{us_rl}/m_{us_rr}	24.4
	Damping coefficient (N.m.s/rad)		
12.	Suspension damper stiffness for front left/ front right	C_{s_fl}/ C_{s_fr}	1570
13.	Suspension damper stiffness for rear left/ rear right	C_{s_rl}/ C_{s_rr}	1760
14.	Tire damper stiffness for front left/ front right	C_{t_fl}/ C_{t_fr}	100
15.	Tire damper stiffness for rear left/ rear right	C_{t_rl}/ C_{t_rr}	100
16.	Front tire cornering stiffness	$C\alpha f$	40000
17.	Rear tire cornering stiffness	$C\alpha r$	40000
	Stiffness coefficient (N.m/rad)		
18.	Spring stiffness of suspension front left/ front right	K_{s_fl}/ K_{s_fr}	20600
19.	Spring stiffness of suspension rear left/ rear right	K_{s_rl}/ K_{s_rr}	15200
20.	Tire stiffness front left / front right	K_{t_fl}/ K_{t_fr}	138000

21.	Tire stiffness rear left / rear right	K_{t_rl}/ K_{t_rr}	138000
22.	Stiffness of anti-roll bars for front suspension	K_{af}	6659
23.	Stiffness of anti-roll bars for rear suspension	K_{ar}	6659
	Moments (kg.m^2)		
24.	Sprung mass moment of inertia about roll axis (x	I_{xx}	300
25.	Sprung mass product of inertia about roll and yaw axes (x-z axis)	I_{xz}	15
26.	Sprung mass moment of inertia about pitch axis (y axis)	I_{yy}	1058.4
27.	Vehicle moment of inertia about yaw axis (z axis)	I_{zz}	1087.8
	Others		
28.	Gravitational acceleration	g	9.82 m/s2
29.	Brake friction coefficient	μ	0.85
30.	Overall steering ratio	OSR	20

Appendix B. Nomenclature

Symbol	Variable
a, b	Distance from vehicle CG to front & rear axle [m]
a_x, a_y	longitudinal and lateral accelerations at center of gravity (CG) of vehicle [m/s^2]
$B, C, D, E, S_h,$ S_v	Pacejka tire parameters
C_{si}	Suspension damper coefficient for the ith corner [N.s/m]
C_{ti}	Tire damping coefficient for ith corner [N.s/m]
$C_{\alpha f}, C_{\alpha r}$	Cornering stiffnesses of front & rear tires [N.m.s/rad]
d	Half of the wheel track [m]
F_{ai}	Active suspension force at the ith corner [kN]
F_{nzi}	Normal Force at the ith tire[kN]
F_{szi}	Vertical Suspension force on the ith corner [kN]
F_{tzi}	Vertical tire force on the ith corner [kN]
F_{xi}	Longitudinal tire force on the ith corner [kN]
F_{yi}	Lateral tire force on the ith corner [kN]
g	Gravitational acceleration [m/s^2]
h_{cg}	Vehicle centroid- to- ground height [m]
h_s	Vehicle focused mass to roll or pitch axle [m]
I_{xx}, I_{yy}, I_{zz}	Mass moments of inertia of the vehicle sprung mass [Kg.m^2]
I_{xy}, I_{xz}, I_{yz}	Products of inertia of the vehicle sprung mass [Kg.m2]

Symbol	Variable
I_w	Wheel moment of inertia about the spin axis [kg.m^2]
K_{af}, K_{ar}	Stiffness of anti-roll bars for front & rear suspensions [N.m/rad]
K_{si}	ith Suspension spring stiffness [N/m]
K_{ti}	ith Tire stiffness [N/m]
k_{us}	Understeer coefficient/ gradient [deg/g]
m	Total vehicle mass [kg]
M_{ESC}	ESC corrective yaw moment [N.m]
M_{TVS}	TVS corrective yaw moment [N.m]
MF	Gain factor
m_s	Vehicle sprung mass [kg]
m_{usi}	Vehicle unsprung mass at the ith corner [kg]
R_w	Dynamic wheel radius [m]
T_b	Braking torque [N.m]
T_{bf}	Front wheel braking torque [N.m]
T_d	Driving torque [N.m]
T_{df}	Front wheel driving torque [N.m]
V_{wxi}	Wheel velocity at ith corner [m]
$\dot{x}$	Vehicle speed in the longitudinal direction[m/s]
$\dot{y}$	Vehicle speed in the lateral direction [m/s]
z_s	Sprung mass vertical displacement from the equilibrium position [m]
$\dot{z}_s$	Sprung mass vertical velocity [m/s]
Z_{usi}	Unsprung mass vertical displacement ith [m]
$\dot{Z}_{usi}$	Unsprung mass vertical velocity ith [m/s]
α_i	Sideslip angle of the ith tire [rad]
β	Sideslip angle of the vehicle at the CG [rad]
γ	Camber angle [rad]
δ_c	Corrective steering angle added by active steering [rad]
δ_d	Steering angle by driver [rad]
δ_f	Front steering angle at wheels [rad]
θ, ϕ, ψ	Sprung mass angular displacements (roll, pitch and yaw) [rad]
$\dot{\theta}, \dot{\phi}, \dot{\psi}$	Sprung mass angular velocities (rates) (roll, pitch and yaw) [rad/s]
$\ddot{\theta}, \ddot{\phi}, \ddot{\psi}$	Sprung mass angular accelerations (roll, pitch and yaw) [rad/s^2]
λ	Tire longitudinal slip ratio [%]
μ	Brake friction coefficient
ω_w	Angular velocity of wheel [rad/s]
i	Front left, front right, rear left, rear right corners

References

[1] Chen W, Xiao H, Chu C, Zu JW., Hierarchical control of automotive electric power steering system and anti-lock brake system: theory and experiment. International journal of vehicle design, 59(1), pp.23-43,2012

[2] Ahangarnejad, ARASH Hosseinian., Integrated Control of Active Vehicle Chassis Control Systems., PhD diss., Ph. D. Dissertation. Politecnico di Milano. Milan, Italy, 2018.

[3] Junjie, H., Integrated *vehicle dynamics control using active steering, driveline and braking* (Doctoral dissertation, Ph. D. Dissertation, University of Leeds, Leeds)., 2005.

[4] Farag, Rana Raouf Hasan., Active neuro-fuzzy integrated vehicle dynamics controller to improve the vehicle handling and stability at complicated maneuvers., PhD diss., Universidad Carlos III de Madrid, 2013.

[5] Dangor, M., Dahunsi, O.A., Pedro, J.O., Ali, M.M., Evolutionary algorithm-based PID controller tuning for nonlinear quarter-car electrohydraulic vehicle suspensions. *Nonlinear dynamics*, *78*(4), pp.2795-2810, 2014.

[6] Elmarakbi, A., Rengaraj, C., Wheatley, A., Elkady, M., The influence of electronic stability control, active suspension, driveline and front steering integrated system on the vehicle ride and handling. Global Journal of Research in Engineering.,13(1), 2013.

[7] Chen, W., Xiao, H., Liu, L., Zu, J.W., Zhou, H., Martínez-Alfaro, H., Integrated control of vehicle system dynamics: theory and experiment. Advances in Mechatronics., 2011.

[8] Nagai, M., Shino, M., Gao, F., Study on integrated control of active front steer angle and direct yaw moment. *JSAE review*, *23*(3), pp.309-315, 2002.

[9] Wei, Jiang, Yu Zhuoping, Zhang Lijun., Integrated chassis control system for improving vehicle stability., *2006 IEEE International Conference on Vehicular Electronics and Safety*, pp. 295-298., 2006.

[10] Karbalaei R, Ghaffari A, Kazemi R, Tabatabaei SH., Design of an integrated AFS/DYC based on fuzzy logic control., 2007 IEEE International Conference on Vehicular Electronics and Safety (pp. 1-6). ,2007.

[11] Zhang L, Pan F, Wang F., Simulation on Automobile Handling and Stability Based on Combination Control., 2009 International Conference on Measuring Technology and Mechatronics Automation 2009 Apr 11, Vol. (2), pp. 347-350. ,2009.

[12] Hu, Aijun, Fuying He., Variable structure control for active front steering and direct yaw moment., *2011 2nd International Conference on Artificial Intelligence, Management Science and Electronic Commerce (AIMSEC)*, pp. 3587-3590. IEEE, 2011.

[13] Hu, Aijun, Baozhan Lv., Study on mixed robust control for integrated active front steering and direct yaw moment., 2010 IEEE International Conference on Mechatronics and Automation, pp. 29-33., 2010.

[14] Cheng, S., Li, L., Mei, M. M., Nie, Y. L., Zhao, L., Multiple-objective adaptive cruise control system integrated with DYC. IEEE Transactions on Vehicular Technology, 68(5), pp.4550-4559, 2019.

[15] Mousavinejad, E., Han, Q.L., Yang, F., Zhu, Y., Vlacic, L., Integrated control of ground vehicles dynamics via advanced terminal sliding mode control., *Vehicle System Dynamics*, *55*(2), pp.268-294, 2017.

[16] Ahangarnejad, A. H., Melzi, S., Ahmadian, M., Integrated Vehicle Dynamics System through Coordinating Active Aerodynamics Control, Active Rear Steering, Torque Vectoring and Hydraulically Interconnected Suspension. International Journal of Automotive Technology, 20(5), 903-915., 2019.

[17] Termous, H., Shraim, H., Talj, R., Francis, C., Charara, A., Coordinated control strategies for active steering, differential braking and active suspension for vehicle stability, handling and safety improvement. Vehicle System Dynamics, 57(10), pp.1494-1529, 2019.

[18] Zhao, J., Wong, P.K., Ma, X., Xie, Z., Chassis integrated control for active suspension, active front steering and direct yaw moment systems using hierarchical strategy. Vehicle System Dynamics, 55(1), pp.72-103, 2017.

[19] Elhefnawy, A., A. M. Sharaf, H. Ragheb, S. Hegazy., Coordinated Chassis Control Based on Vehicle Lateral Acceleration Using Fuzzy Logic Control., In International Conference on Aerospace Sciences and Aviation Technology, vol. 17, no. AEROSPACE SCIENCES & AVIATION TECHNOLOGY, ASAT-17–April 11-13, 2017, pp. 1-19. The Military Technical College, 2017.

[24] Rengaraj, Chandrasekaran., Integration of active chassis control systems for improved vehicle handling performance., PhD diss., University of Sunderland, 2012.

[25] Soltani, Amirmasoud., Low cost integration of electric power-assisted steering (EPAS) with enhanced stability program (ESP)., PhD diss., Cranfield University, 2014.

[26] Elhefnawy, A., A. M. Sharaf, H. M. Ragheb, S. M. Hegazy., Integrated vehicle chassis control based on direct yaw moment and active front steering. In *The International Conference on Applied Mechanics and Mechanical Engineering*, vol. 17, no. 17th International Conference on Applied Mechanics and Mechanical Engineering, pp. 1-19. Military Technical College, 2016.

[27] Shi, PeiCheng, Qi Zhao, RongYun Zhang, Li Ye., The Simulation of Tire Dynamic Performance Based on" Magic Formula"., *2017 2nd International Conference on Automation, Mechanical Control and Computational Engineering (AMCCE 2017)*. Atlantis Press, 2017.

[28] Karogal, I., Independent Torque Distribution Management Systems for Vehicle Stability Control., M.Sc. diss., Clemson University,2008.

[29] Griffin, Joseph W., Influences of drive torque distribution on road vehicle handling and efficiency., PhD diss., University of Nottingham, 2015.

[30] Hsu, L. Y., Vehicle rollover prediction system using states observers., PhD diss., MA thesis, Department Mechanical Engineering, National Chiao Tung University, Hsinchu, Taiwan, 2006.

تصميم وتقييم جهاز التحكم النشط القائم على السرعة للتحكم في المركبة من أجل الاستقرار الجانبي

الملخص

تم تقديم نظام تحكم فعال ومتكامل في المركبة يطبق التحكم المنطقي الضبابي (FLC) . يدمج النظام ثلاثة أنظمة تحكم نشطة بالمركبة متوفرة تجارياً ، وهي التوجيه الأمامي النشط (AFS) والتحكم الإلكتروني بالثبات (ESC) ونظام توجيه عزم الدوران (TVS) بهدف تعزيز التعامل مع المركبة واستقرار المنعطفات ومنع الانقلاب. تم إنشاء نموذجين مختلفين للمركبة لمحاكاة السلوك الديناميكي للنظام مع أو بدون وحدة تحكم التكامل المقترحة، أي نموذج ديناميكي للمركبة ١٤ DOF-بخصائص الإطارات غير الخطية ونموذج مرجعي للدراجات. DOF٢-تم استخدام النموذج الأخير لإخراج هدف التحكم المطلوب لكل من معدل ياو وزاوية الانزلاق الجانبية لجسم المركبة. تم إجراء المحاكاة في بيئة برنامج MATLAB / SIMULINK. تم التحقق من فعالية النظام بتطبيق خمس مناورات مختلفة لاختبار المنعطفات بسرعات أمامية مختلفة للمركبة تبلغ ١٠ و٢٠ و٣٠ م / ث. مناورات اختبار المحاكاة هي: الخطوة، والانعطاف على شكل حرف J ، وتغيير الحارة المفرد، وجيب مع الاستقرار، وخطاف الصيد. تُظهر النتائج أنه من أجل تعزيز الثبات، يكون نظام AFS أكثر فاعلية في السرعات المنخفضة للمركبة مع انخفاض فعاليته مع زيادة السرعة. تم العثور على كل من ESC و TVS لتكون فعالة بنفس القدر في السرعات المتوسطة والعالية. ومع ذلك، نظرًا للطبيعة التدخلية لـ ESC ، تعتبر TVS هي آلية التحكم المفضلة في الاستقرار. تم استخدام معيار الاستقرار القائم على السرعة لتعيين سلطة التحكم في الاستقرار وضمان الانتقال السلس لسلطة التحكم بين الأنظمة المتكاملة، وبالتالي تقديم نظام قوي للتحكم في الهيكل. (ICC)